

# **INCORPORATION OF CADMIUM IONS AND CADMIUM SULFIDE PARTICLES INTO SOL-GEL ZIRCONIUM PHOSPHATE**

## **Synthesis, thermal behavior and X-ray characterization**

*C. Ferragina, P. Cafarelli and R. Di Rocco*

CNR Istituto di Metodologie Avanzate Inorganiche-IMAI, via Salaria Km. 29300,  
00016 Monterotondo, Rome, Italy

(Received June 16, 2000; in revised form October 30, 2000)

### **Abstract**

The inorganic ion-exchanger  $\alpha$ -zirconium phosphate was synthesized by the sol-gel method and its properties relating to the exchange of  $\text{Cd}^{2+}$  and the intercalation of CdS particles were studied. The  $\text{Cd}^{2+}$ -exchange process is a fast process and the material obtained exhibits an increased interlayer distance  $d$  with respect to its precursor (9.56 vs. 7.56 Å). The resulting Cd-containing material was exposed to a  $\text{H}_2\text{S}$  gas flow to give CdS particles in the exchanger. The zirconium phosphate containing CdS particles still possesses a layered structure, with a pattern almost identical to that of the initial ion-exchanger precursor. Moreover, the material may exchange further  $\text{Cd}^{2+}$  and hence lead to a higher CdS particle content. The thermal behavior of this ion-exchangers containing  $\text{Cd}^{2+}$  or CdS particles was studied.

**Keywords:** intercalation compounds, ion-exchanger, layered composite, thermal behavior

### **Introduction**

There has recently been increasing interest in the study of the ion-exchangers  $\alpha$ - and  $\gamma$ -zirconium and  $\gamma$ -titanium phosphates, in consequence of their ability to exchange metal ions [1] and to intercalate polar molecules between the layers [2]. These materials are obtained in amorphous or crystalline form, depending on the method of synthesis.  $\alpha$ -Zirconium phosphate,  $\alpha\text{-Zr}(\text{HPO}_4)_2 \cdot \text{H}_2\text{O}$  ( $\alpha\text{-ZrP}$ ,  $d=7.56$  Å), was initially prepared as a gel [3]; then, in 1964, Clearfield and Stynes synthesized a crystalline material [4]. The synthesis procedure has been modified over the years, and  $\alpha\text{-ZrP}$  can nowadays be prepared in amorphous or crystalline form [5], as a single crystal [6] or as a sol-gel [7] (SGZrP). The terminology 'sol-gel' describes a broad class of processes in which a solid phase is formed through a gelatinous phase of a colloidal suspension. The main advantages of this process include the control of hydrolysis, operation at low temperatures, which minimizes evaporation losses and avoids phase separation, and better homogeneity for multicomponent materials.

$\alpha$ -ZrP prepared by the traditional method [5] has been widely studied with regard to its property of exchanging cations. The exchange of transition metal ions [8, 9] for heterogeneous catalysis is of particular interest [10]. One of the most studied properties is the ability of  $\alpha$ -ZrP to act as a host material in the intercalation reactions of a variety of organic and polar guest molecules (amines, alcohols, diols and thiols) [11]. Recent studies have been devoted to investigations of the inclusion of particles acting as semiconductors, such as CdS, CdSe and ZnS in the zeolites [12] or  $\alpha$ -ZrP [13], or the mixed phase [14]. The goal was to establish the size of the metal sulfide particles.

The inclusion of CdS particles in the  $\gamma$ -phase of ZrP was earlier studied [15] with a view to obtaining multifunctional nanocomposite solids. The present work describes the synthesis and physico-chemical characterization of SGZrP used as an ion-exchanger with  $\text{Cd}^{2+}$  and as matrix for the *in situ* formation of CdS particles. The aim was to determine the advantages of using  $\alpha$ -ZrP that has not been prepared by the conventional powder method for a better control of the whole process and for the synthesis of 'specific materials'.

## Experimental procedure

### *Chemicals*

The cadmium acetate dihydrate and iron sulfide were reagent grade products purchased from Aldrich and were used without further purification. All other reagents were Merck p.a. products.

### *Materials*

Crystalline SGZrP was prepared as reported in the literature [7]. The cadmium SGZrP (SGZrPCd) was prepared by ion-exchange, in a batch procedure, between SGZrP and cadmium acetate solution, at 45°C, for different periods of time. In general, samples of 1 mmol of SGZrP were brought into contact with 200 ml of  $5 \cdot 10^{-3}$  mol  $\text{dm}^{-3}$  of cadmium acetate solution, so as to obtain the fully exchanged Cd-Zr phase. After the suspension had been stirred for different periods of time, the solid was recovered by centrifugation and dried in air.

The SGZrP (SGZrPCdS) was obtained by flowing anhydrous  $\text{H}_2\text{S}$  over cadmium SGZrPCd for different periods of time.

### *Physical measurements and chemical analysis*

$\text{Cd}^{2+}$  was determined before and after centrifugation, on a GBC 903 A.A. spectrophotometer. Phosphates were determined colorimetrically [16].

The water content and thermal behavior of each of the obtained materials were determined with a simultaneous TG-DTA Stanton Redcroft 1500 thermoanalyzer, with samples in Pt crucibles, calcined to constant mass in an air flow at a heating rate of  $10^\circ\text{C min}^{-1}$  up to  $1100^\circ\text{C}$ . X-ray powder diffraction was used to study the phase

changes undergone by the materials. This involved monitoring the  $d$  reflection and its harmonics. A Philips diffractometer (model PW 1130/00) was used with Ni-filtered  $\text{CuK}\alpha$  radiation ( $\lambda=1.541 \text{ \AA}$ ). The contents of  $\text{S}^{2-}$  and  $\text{H}^+$  in the materials were determined with a Fisons 1108 elemental microanalyzer.

## Results and discussion

### Materials derived from SGZrP

#### Cadmium uptake

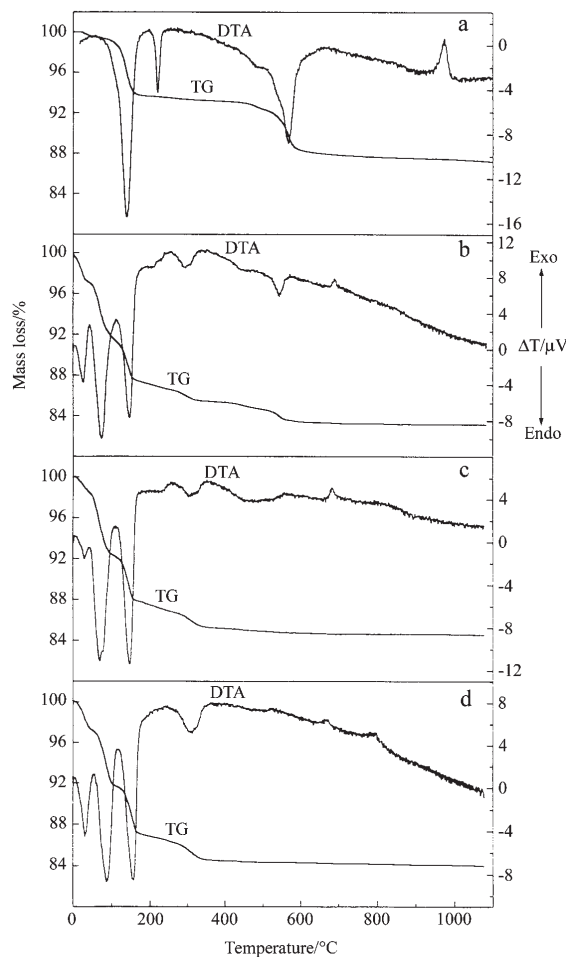
Table 1 reports the chemical composition and the interlayer distance  $d$  of the SGZrPCd materials obtained by ion-exchange, after contact for various periods of time. The Cd uptake was initially fast (as compared with that into  $\gamma$ -ZrP under the same conditions) [15]. After a batch contact time of 15 min between the ion-exchanger and the cadmium acetate solution, half of the hydrogen present in the SGZrP had been substituted by  $\text{Cd}^{2+}$ . A slowdown in the Cd uptake then occurred; the last traces of  $\text{H}^+$  were exchanged increasingly more slowly. An almost fully exchanged compound was obtained after one day of batch contact. The fully exchanged form was obtained after a prolonged batch contact time (2 weeks) or with renewed cadmium acetate solution. The kinetic uptake of  $\text{Cd}^{2+}$  by SGZrP was faster than that by  $\gamma$ -ZrP, although the interlayer distance is smaller (12.26 vs. 7.56  $\text{\AA}$ ). As reported previously [15], the fully exchanged SGZrPCd can be obtained in a shorter time by the hydrothermal method at 80°C for 4 days.

**Table 1** Chemical compositions and interlayer distances of SGZrPCd materials

Time/h	Chemical composition	$d/\text{\AA}$
0.4	$\text{ZrH}_{0.96}\text{Cd}_{0.52}(\text{PO}_4)_2 \cdot 2.70\text{H}_2\text{O}$	7.56–9.56
0.2	$\text{ZrH}_{0.88}\text{Cd}_{0.56}(\text{PO}_4)_2 \cdot 2.84\text{H}_2\text{O}$	7.56–9.56
1	$\text{ZrH}_{0.50}\text{Cd}_{0.75}(\text{PO}_4)_2 \cdot 3.16\text{H}_2\text{O}$	9.56
3	$\text{ZrH}_{0.40}\text{Cd}_{0.80}(\text{PO}_4)_2 \cdot 3.20\text{H}_2\text{O}$	9.56
6	$\text{ZrH}_{0.24}\text{Cd}_{0.88}(\text{PO}_4)_2 \cdot 3.50\text{H}_2\text{O}$	9.56
24	$\text{ZrH}_{0.14}\text{Cd}_{0.93}(\text{PO}_4)_2 \cdot 3.50\text{H}_2\text{O}$	9.56
72	$\text{ZrH}_{0.14}\text{Cd}_{0.93}(\text{PO}_4)_2 \cdot 3.50\text{H}_2\text{O}$	9.56
168	$\text{ZrH}_{0.10}\text{Cd}_{0.95}(\text{PO}_4)_2 \cdot 3.50\text{H}_2\text{O}$	9.56
2 weeks	$\text{ZrCd}(\text{PO}_4)_2 \cdot 4\text{H}_2\text{O}$	9.56

#### Thermal behavior

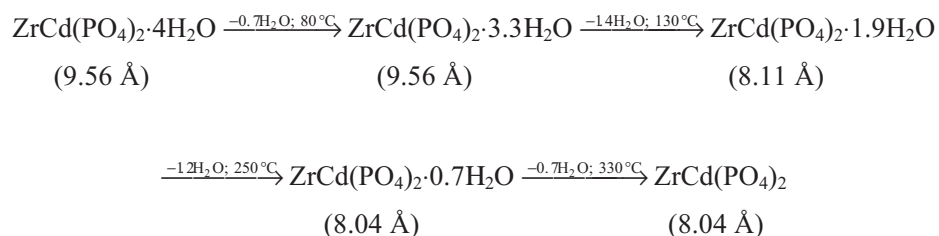
Figure 1 depicts the simultaneous TG-DTA curves of the materials containing Cd in SGZrP, obtained after various periods of time. The TG curves are very similar. Between 25 and 330°C, coordination water is lost. For the materials obtained after batch contact times of 15 and 30 min, water loss is evident in the interval 400–650°C. This



**Fig. 1** TG-DTA curves of a – SGZrP; b – SGZrP in contact with  $\text{Cd}^{2+}$  for 0.2 h; c – SGZrP in contact with  $\text{Cd}^{2+}$  for 1 h; d – SGZrPCd fully exchanged

is due to the condensation of the residual hydrogen of the phosphate groups, which forms pyrophosphates. The  $\text{H}^+$  is exchanged for  $\text{Cd}^{2+}$ , as observed in the material obtained after a batch contact time of 3 h. In the fully exchanged form  $\text{SGZrCd}(\text{PO}_4)_2 \cdot 4\text{H}_2\text{O}$  (SGZrPCd), no water condensation from the phosphate group is observed.

The DTA curves of the Cd-containing materials confirm the TG data, showing endothermic peaks for the water losses. At  $700^\circ\text{C}$ , the exothermic peak relating to the transition of *L*-pyrophosphate groups to  $\alpha$ -cubic pyrophosphate is evident in the materials that have residual hydrogen to be exchanged, while it is absent for the fully exchanged Cd form. It should be noted that in SGZrP this exothermic peak is present at  $980^\circ\text{C}$ .

**Scheme 1** Steps of SGZrPCd dehydration

Scheme 1 reports the dehydration steps, at different temperatures, with the  $d$  value of the fully exchanged form SGZrPCd. The water loss is similar to that for  $\alpha$ -ZrP exchanged with transition metal ions [9]. After each step of water loss, the SGZrPCd was left in air for one day to rehydrate. The dehydration in the first three steps was found to be almost quantitatively reversible ( $\sim 70\%$ ).

**XRD**

The XRD pattern of SGZrPCd exhibits a larger  $d$  than that for its precursor (9.56 vs. 7.56 Å). While the Cd content inside the exchanger is  $\leq 0.70 \text{ mol mol}^{-1}$  SGZrP, two

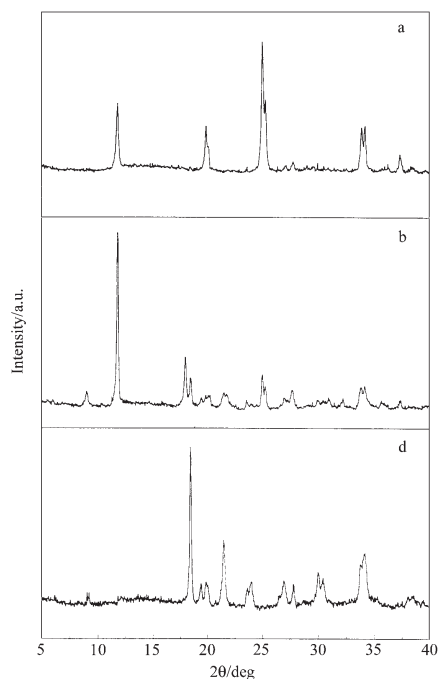


**Fig. 2** XRD at 25°C of a – SGZrP; b – SGZrP in contact with  $\text{Cd}^{2+}$  for 0.2 h; d – SGZrPCd fully exchanged

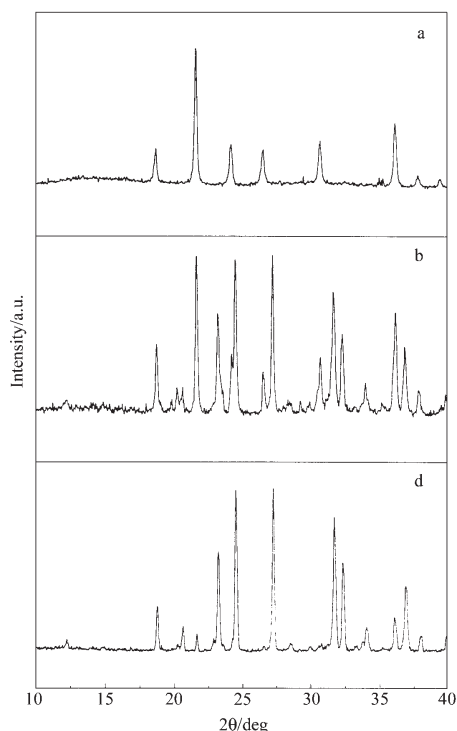


**Fig. 3** XRD at 1100°C of a – SGZrP; b – SGZrP in contact with Cd<sup>2+</sup> for 0.2 h; d – SGZrPCd fully exchanged

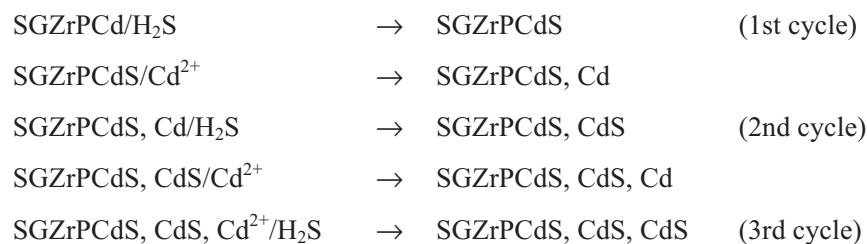
phases with  $d=7.56$  and  $9.56$  Å are observed in the diffractograms. They are related to the initial ion-exchanger and the fully substituted Cd form, respectively. The X-ray diffraction pattern of SGZrPCd was recorded after various dehydration steps and at 700–1100°C. The layered structure was maintained up to 330°C (in this case, the material was slightly amorphous). At 700°C, the patterns typical of Cd–Zr double phosphate were observed on analogy with the Ca–Zr double phosphate reported previously [17]. Figures 2 and 3 display the XRD patterns of SGZrP and the partially and fully exchanged SGZrPCd material at room temperature and at 1100°C, respectively. In the case of the partially exchanged Cd compounds calcined at 1100°C, the diffractograms clearly showed the presence of  $\alpha$ -cubic pyrophosphate and the Cd–Zr double phosphate.

#### *Materials obtained from SGZrPCd with hydrogen sulfide*

##### Synthesis

The general procedure to obtain CdS particles in the interlayer of ZrP prepared as a sol-gel can be summarized as follows: anhydrous H<sub>2</sub>S is flowed for various periods of time (1–30 h) at room temperature over a sample of 1 mmol of SGZrPCd previously

heated at 330°C (TG curve in Fig. 1(d)) for 2 h to achieve complete dehydration. The dehydration is necessary to allow the H<sub>2</sub>S to flow through the layers of the material, even though this dehydration causes a decrease in the interlayer distance of the material from 9.56 to 8.04 Å (Scheme 2). The anhydrous H<sub>2</sub>S is obtained by reacting FeS with HCl and by dehydrating the gas over two columns containing H<sub>2</sub>SO<sub>4</sub> and CaSO<sub>4</sub>. When the gas flows over the white dehydrated SGZrPCd, its color suddenly changes to yellow, which becomes more and more intense as the duration of the H<sub>2</sub>S flow increases. The flowing gas combines with Cd<sup>2+</sup> already exchanged in SGZrP to give yellow CdS particles. The chemical composition of the material obtained after 30 h of H<sub>2</sub>S flow is Zr(CdS)<sub>0.9</sub>Cd<sub>0.1</sub>(H<sub>0.72</sub>PO<sub>4</sub>)<sub>2</sub>·2.7H<sub>2</sub>O (SGZrPCdS). When the experiment was performed with a shorter H<sub>2</sub>S flow time (e.g. 8 h), the quantity of S<sup>2-</sup> in the SGZrPCd was quite similar to that observed after gas flow for 30 h. This behavior reveals a good affinity between Cd<sup>2+</sup> and S<sup>2-</sup> to give CdS particles in the SGZrP host matrix. Table 2 shows the S and H contents of the SGZrPCdS materials obtained after various H<sub>2</sub>S flow times.



#### Scheme 2

**Table 2** Percentage masses of H and S in the SGZrPCdS materials obtained (after a H<sub>2</sub>S flow) for various periods of time

Time of H <sub>2</sub> S flow/h	H/%	S/%
5	0.78	3.39
10	0.74	7.19
15	0.71	7.22
30	0.76	7.39

#### Thermal behavior

The TG-DTA curves of the materials listed in Table 2 are quite similar, except the first one. As observed in Fig. 4a for the SGZrPCdS material obtained after a H<sub>2</sub>S flow for 30 h, the TG curve reveals an evident water loss in two steps between 25 and 220°C: 1 molecule was lost at 25–80°C and 1.7 molecules at 80–220°C due to the different strengths of water bonding with the material. The large loss which starts at 230 and stops at 620°C is related to the combustion and elimination of S ions. The final small loss may be ascribed to the H<sup>+</sup> replaced by the Cd<sup>2+</sup> from the phosphate groups

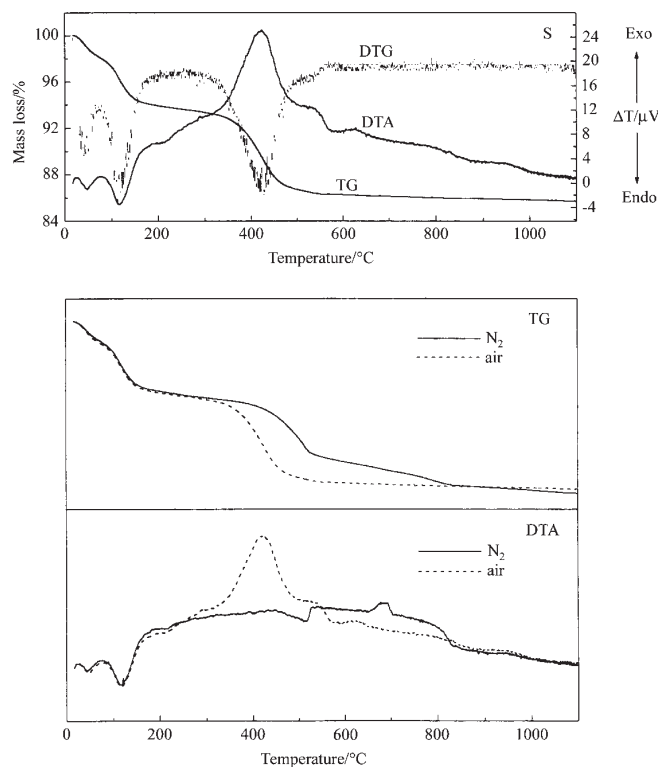


**Fig. 4** TG-DTG-DTA of *s* – SGZrPCdS (on the top); TG-DTA curves of SGZrPCdS under air (dotted line) and N<sub>2</sub> flow (dark line) (on the bottom)

during CdS formation. The DTA curve is in agreement with the endothermic peaks for the water loss and the exothermic peaks for S ions elimination. Indeed, three exothermic peaks are noted at 400°C (largest), 530 and 620°C (smallest). It is presumed that the CdS particles are bonded differently in the exchanger, and thus the S<sup>2-</sup> is burned and eliminated at different temperatures. The DTG curve clearly confirms all the losses, as shown in Fig. 4a. As concerns the small exothermic peaks at 530 and 620°C, two losses at the same temperatures are evident in the DTG curve, which cannot be clearly distinguished in the corresponding TG curve. To eliminate any interpretation problem due to the S<sup>2-</sup> elimination at these temperatures, thermal treatment was performed in a N<sub>2</sub> flow. Figures 4b and 4c depict the TG-DTA curves of the SGZrPCdS material obtained in air and a N<sub>2</sub> flow, respectively. The two TG curves show that the water loss occurs both in air and in a N<sub>2</sub> environment. The initial S<sup>2-</sup> elimination in N<sub>2</sub> occurs at a temperature ~100°C higher than that in air; immediately afterwards, a continuous loss is observed up to 850°C. The DTA curves do not show any differences in water loss in the two atmospheres. If the experiment is performed in N<sub>2</sub>, there are endothermic peaks instead of exothermic peaks for S<sup>2-</sup> elimination. At



680°C, there is an exothermic peak in the DTA curve obtained under a N<sub>2</sub> flow. This can be attributed to a phase transition of the material.

### XRD

Figure 5 compares the XRD pattern of SGZrPCdS with that of SGZrP. The diffractograms are very similar. SGZrPCdS has a layered structure, with the *d* values decreased by ~2 Å with respect to that of SGZrPCd (7.56 vs. 9.56 Å). When H<sub>2</sub>S

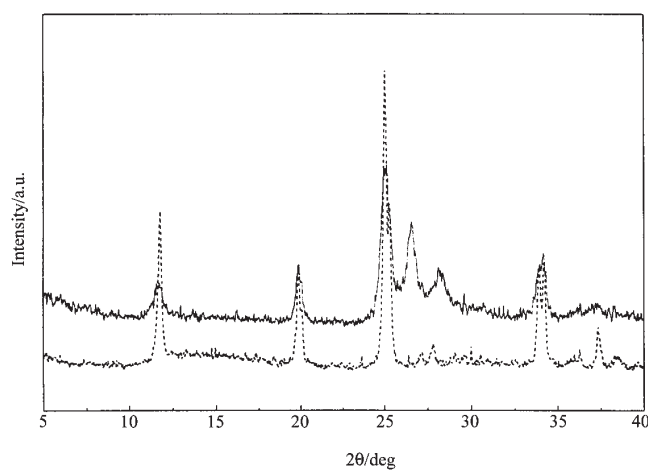


**Fig. 5** XRD at 25°C of SGZrP (dotted line) and SGZrPCdS (dark line) for comparison

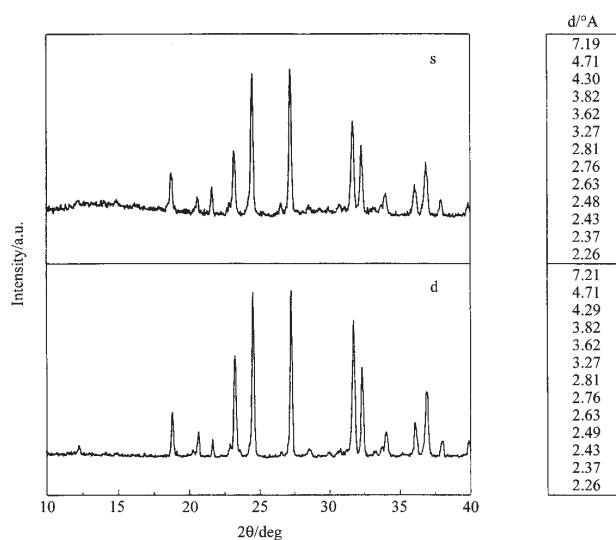


**Fig. 6** XRD at 1100°C of s – SGZrPCdS and d – SGZrPCd materials heated at 1100°C, and the relative values in the Table

flows over SGZrPCd, 'reversion' to the initial host SGZrP form is observed in the XRD. This means that S combines with  $\text{Cd}^{2+}$  to give CdS particles inside the exchanger and the H of the  $\text{H}_2\text{S}$  gas can replace the free charge left from the  $\text{Cd}^{2+}$ . The material obtained is characterized by its XRD pattern after heating at the temperature corresponding to the losses indicated in the thermoanalytical curves. The materials were heated to 40, 120 and 220°C. A layered structure similar to that at room temperature was observed up to 220°C. At 450°C, the material was amorphous. At 700°C, once the  $\text{S}^{2-}$  had been eliminated, new reflections appeared. At 1100°C, these reflections were the same as those observed in the case of SGZrPCd at the same temperature; both materials gave Cd–Zr double phosphate [17]. The diffractograms and the  $d$  values of SGZrPCd and SGZrPCdS heated at 1100°C are shown in Fig. 6.  $\text{S}^{2-}$  elimination was confirmed by microanalyses of the material calcined at 400–550°C and by the color of the calcined material, which became a lighter yellow (at 400°C) and then white (at 600°C).

#### Thermal behavior and XRD of SGZrPCdS as ion-exchanger

As mentioned above SGZrPCdS exhibited a 'reversion' in the XRD pattern due to the initial SGZrP phase. For this reason, the material was reused as an ion-exchanger for 'other'  $\text{Cd}^{2+}$  to obtain an increased number of CdS particles. 1 mmol of SGZrPCdS was maintained in contact with a  $5 \cdot 10^{-3}$  mol  $\text{dm}^{-3}$  solution of cadmium acetate, in batch at 60°C for a week. The solid was recovered by centrifugation and dried in air. After dehydration at 220°C, it was treated in a  $\text{H}_2\text{S}$  gas flow. This process (batch contact with  $\text{Cd}^{2+}$  solution and a  $\text{H}_2\text{S}$  gas flow) was repeated three times. Scheme 2 details the experiments performed and the materials obtained. The atomic adsorption and microanalysis measurements showed increases in the contents of  $\text{Cd}^{2+}$  and  $\text{S}^{2-}$  with respect to the initial SGZrPCdS. These data are reported in Table 3.

**Table 3** Percentage masses of H and S;  $\text{Cd}^{2+}$  mol  $\text{mol}^{-1}$  SGZrP, in the SGZrPCdS materials obtained (in various cycles)

Materials	H/%	S/%	$\text{Cd}^{2+}$
SGZrPCdS	0.76	7.39	1
SGZrPCdS, CdS	0.55	9.81	1.44
SGZrPCdS, CdS, CdS	0.39	12.77	1.60

Figures 7 and 8 present the TG-DTA curves and X-ray diffractograms for the materials obtained after the above cycles. The TG and DTA curves in Figs 7b and c demonstrate that, when the materials were subjected to a  $\text{H}_2\text{S}$  flow, an increase in area of the exothermic peak at 610°C was noted. This increase might be due either to the increased formation of CdS particles (obtained after several cycles) or to a phase transition, including oxidation. Oxidation is justified by a mass increase at 610°C in the TG curve. This problem remains open. However, the X-ray diffractograms at 610 and 1100°C are very different from those for SGZrPCdS at the same temperature. For the SGZrPCdS obtained after various cycles (Figs 7d and 7e) the TG-DTA curves are

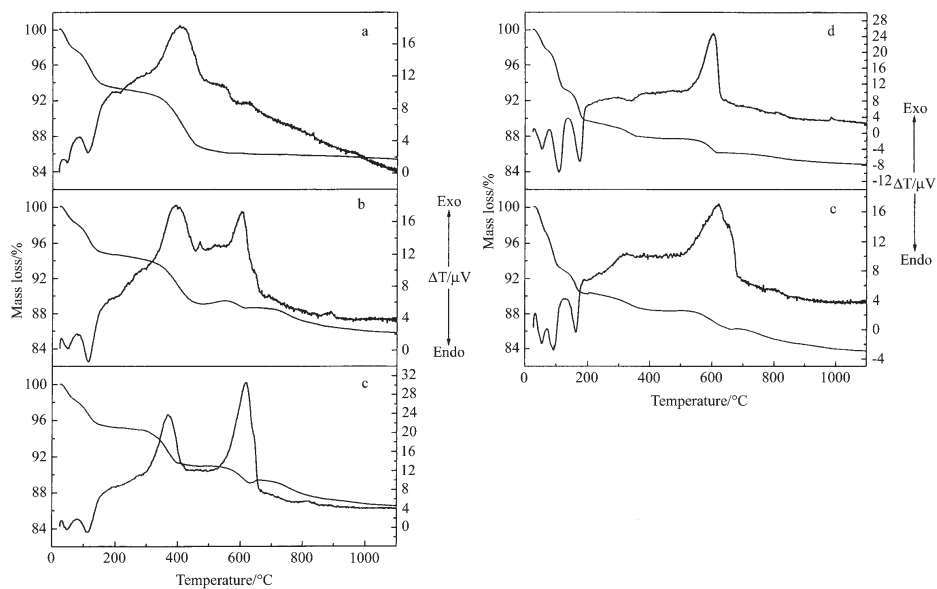


**Fig. 7** TG-DTA curves of a – SGZrPCdS; b – SGZrPCdS, CdS; c – SGZrPCdS, CdS, CdS; d – SGZrPCdS, Cd; e – SGZrPCdS, CdS, Cd (Scheme 2 for the symbols)

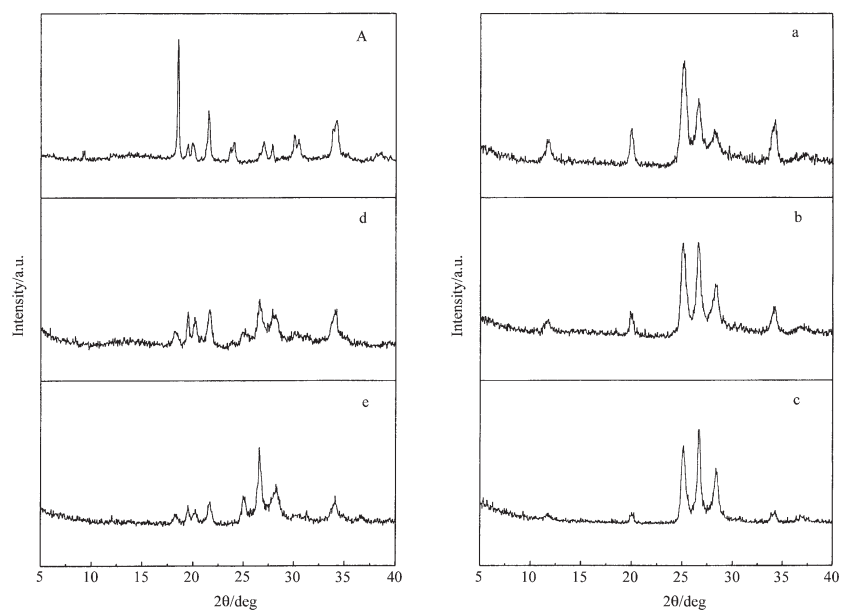


**Fig. 8** XRD of A – SGZrPCd; a – SGZrPCdS; b – SGZrPCdS, CdS; c – SGZrPCdS, CdS, CdS; d – SGZrPCdS, Cd; e – SGZrPCdS, CdS, Cd (Scheme 2 for the symbols)

very similar to that for SGZrPCd (Fig. 1d), except for the exothermic peak at 610°C (relating to the presence of CdS particles). The X-ray patterns for the initial material [(A) SGZrPCd] and for the materials obtained after various cycles [(d) SGZrPCdS, Cd and (e) SGZrPCdS, CdS, Cd] are reported on the left side of Fig. 8. In this figure, the reflections of materials (d) and (e) are quite similar to those of material (A). The X-ray patterns relating to SGZrPCdS (a) and to the materials obtained after the second and third cycles [(b) SGZrPCdS, CdS; and (c) SGZrPCdS, CdS, CdS] are reported on the right side of Fig. 8. It is evident that the three materials furnish the same diffractograms. In this way, it has been demonstrated that SGZrPCdS can be used as an ion-exchanger to increase both the Cd<sup>2+</sup> uptake and the CdS formation inside the host matrix.

## Conclusions

Cd<sup>2+</sup> can be inserted between the layers of SGZrP ( $\alpha$ -zirconium phosphate synthesized by the sol-gel method) by ion-exchange at 45°C. The TG-DTA curves of SGZrPCd show losses in four steps between 25 and 330°C, due to coordination water. The XRD pattern reveals an increase in  $d$  with respect to its precursor (9.56 vs. 7.56 Å). After full dehydration,  $d$  has decreased by 1.52 Å. It is possible to rehydrate the dehydrated material up to ~70% in air.

When anhydrous H<sub>2</sub>S is flowed over the white SGZrPCd, its color suddenly changes to yellow for the gas which reacts with Cd<sup>2+</sup> to give CdS particles. The TG-DTA curves of SGZrPCdS indicate water loss up 220°C. A considerable loss between 230 and 620°C, in three steps, is related to the combustion and elimination of the S<sup>2-</sup> probably due to differently bonded CdS particles between the ZrP layers. Three exothermic peaks in this range of temperature confirm this. The XRD pattern of SGZrPCdS demonstrates a layered structure, almost identical to that of the precursor SGZrP. The 'reversion' to SGZrP suggested the re-use of the SGZrPCdS obtained as an ion-exchanger of more Cd<sup>2+</sup> in order to increase the number of CdS particles inside it. The TG-DTG-DTA, XRD, atomic absorption spectrophotometry and microanalysis of the materials obtained after the treatments confirmed the increased number of CdS particles.

\* \* \*

We thank Dr. L. Petrilli for the microanalysis measurements (CNR Microanalytical Service of Area della Ricerca di Roma) and Dr. L. Avaldi for helpful suggestions.

## References

- 1 A. Clearfield, *Inorganic Ion-Exchange Materials*, Ed. A. Clearfield, CRC Press, Boca Raton, FL, 1981, Chap. 1, p. 20 and references therein.
- 2 G. Alberti and U. Costantino, *Inclusion Compounds*, Eds. J. L. Atwood, J. E. D. Davies and D. D. MacNicol, Chap. 5, University Press, New York 1982, p. 136.

- 3 A. Clearfield, A. Oskarsson and C. Oskarsson, *Ion Exch. Member.*, 1 (1972) 91; K. A. Kraus and H. O. Phillips, *J. Am. Chem. Soc.*, 78 (1956) 644.
- 4 A. Clearfield and J. A. Stynes, *J. Inorg. Nucl. Chem.*, 26 (1964) 117.
- 5 G. Alberti and E. Torracca, *J. Inorg. Nucl. Chem.*, 30 (1967) 317.
- 6 A. Clearfield and G. Smith, *Inorg. Chem.*, 8 (1969) 431.
- 7 J. Livage, H. Benhamza, P. Barboux, A. Bouhaouss and F. A. Josien, *J. Mat. Chem.*, 1 (1991) 681.
- 8 A. Clearfield and J. M. Kalnins, *J. Inorg. Nucl. Chem.*, 38 (1976) 849.
- 9 S. Allulli, C. Ferragina, A. La Ginestra, M. A. Massucci and N. Tomassini, *J. Chem. Soc. Dalton Trans.*, (1977) 1879.
- 10 C. Ferragina, A. La Ginestra, M. A. Massucci, P. Patrono, P. Giannoccaro, F. Nobile and G. Moro, *J. Mol. Catal.*, 53 (1989) 349.
- 11 G. Alberti and U. Costantino, *Intercalation Chemistry*, Eds. M. S. Whittingham and A. J. Jacobson, Academic Press, 1982, p. 147.
- 12 W. Chen, Y. Xu, Z. Lin, Z. Wang and L. Lin, *Solid State Comm.*, 105 (1998) 129.
- 13 A. G. Cao, L. K. Rabenberg, C. M. Nunn and T. E. Mallouk, *Chem. Mat.*, 3 (1991) 149.
- 14 T. Cassageau, G. B. Hix, D. J. Jones, P. Maireles-Torres, M. Rhomari and J. Roziere, *J. Mater. Chem.*, 4 (1994) 189.
- 15 C. Ferragina and R. Di Rocco, *Mater. Res. Bull.*, 34 (1999) 1981.
- 16 G. Alberti, U. Costantino and E. Torracca, *J. Inorg. Chem.*, 28 (1966) 225.
- 17 S. Allulli, C. Ferragina, A. La Ginestra, M. A. Massucci, N. Tomassini and A. A. G. Tomlinson, *J. Chem. Soc.*, (1976) 2115; C. Bettinali, A. La Ginestra and M. Valigi, *Atti Accad. Naz. Lincei, Sez. 8*, 1962, p. 472.